

High Spin Molecules: $[\text{Mn}_{12}\text{O}_{12}(\text{O}_2\text{CCH}_2\text{Cl})_{16}(\text{H}_2\text{O})_4]$ and the One-electron Reduction Product $[\text{PPh}_4][\text{Mn}_{12}\text{O}_{12}(\text{O}_2\text{CCH}_2\text{Cl})_{16}(\text{H}_2\text{O})_3]$

Hui-Lien Tsai,* Tyn-Yih Jwo, Gene-Hsiang Lee,† and Yu Wang‡

Department of Chemistry, National Cheng Kung University, Tainan, Taiwan 70101, R.O.C.

‡Instrumentation Center, College of Science, National Taiwan University, Taipei, Taiwan 10601, R.O.C.

(Received December 6, 1999; CL-991027)

The complex of $[\text{Mn}_{12}\text{O}_{12}(\text{O}_2\text{CCH}_2\text{Cl})_{16}(\text{H}_2\text{O})_4]$ was reduced by PPh_4I to give a reduced complex $[\text{PPh}_4][\text{Mn}_{12}\text{O}_{12}(\text{O}_2\text{CCH}_2\text{Cl})_{16}(\text{H}_2\text{O})_3]$. Crystal structures of both complexes were determined by the X-ray method. The dc magnetic susceptibility measurements indicate that the neutral and reduced complexes are high spin species.

Single-molecule magnets (SMM) are attracting extensive attention because they represent nanoscale magnetic particles of a well-defined size.¹⁻⁶ They display sluggish magnetization relaxation phenomena such as magnetization hysteresis loops and frequency-dependent out-of-phase alternating current (AC) magnetic susceptibility. The remarkable magnetic properties of a SMM arise from the SMM's high-spin ground state (S) split by a large negative axial zero-field splitting (D) which results in an anisotropy energy barrier of $KV = |D|\hat{S}^2$.⁷ The first SMM reported was $[\text{Mn}_{12}\text{O}_{12}(\text{O}_2\text{CCH}_3)_{16}(\text{H}_2\text{O})_4] \cdot 2\text{HOAc} \cdot 4\text{H}_2\text{O}$ (**1**) with $S = 10$ ground state and a negative zero-field splitting of -0.5 cm^{-1} .^{1,2,5} The one electron reduction complex $[\text{PPh}_4][\text{Mn}_{12}\text{O}_{12}(\text{O}_2\text{CCH}_2\text{H}_5)_{16}(\text{H}_2\text{O})_4]$ (**2**) was also reported to have $S = 19/2$ ground state and behave as a SMM.^{2,6} We herein describe the preparation and X-ray structures of two new SMMs, $[\text{Mn}_{12}\text{O}_{12}(\text{O}_2\text{CCH}_2\text{Cl})_{16}(\text{H}_2\text{O})_4] \cdot 3\text{CH}_2\text{Cl}_2 \cdot 2\text{H}_2\text{O}$ (**3**) and its reduced $[\text{PPh}_4][\text{Mn}_{12}\text{O}_{12}(\text{O}_2\text{CCH}_2\text{Cl})_{16}(\text{H}_2\text{O})_3] \cdot 2\text{CH}_2\text{Cl}_2 \cdot 2\text{H}_2\text{O}$ (**4**) that differ in their space group and the positioning of their H_2O ligands on the Mn_{12} complexes.

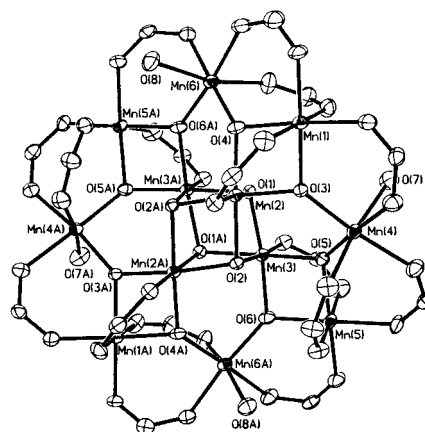
The acetate derivative, complex **3** may be synthesized through the removal of $\text{CH}_3\text{CO}_2\text{H}$ as toluene azeotrope from the reaction of complex **1** with excess ClH_2CCOOH . The neutral complex **3** shows a chemically reversible reduction at 0.53 V vs ferrocene/ferrocenium. Reduction of **3** with PPh_4I yields the stable complex **4**. Both **3** and **4** have been recrystallized from a mixture of dichloromethane and hexane, and afforded suitable crystals for the X-ray crystal structure analysis.

X-Ray data were measured on an Enraf-Nonius CAD4 and a Bruker-axs, SMART CCD diffractometer with graphite monochromatized Mo-K α radiation for complexes **3** and **4**, respectively.⁸

The ORTEP plot of the complex **3** is shown in Figure 1(a). The structure of complex **3** is quite similar in many respects to complex **1**.⁹ Complex **3** possesses a $[\text{Mn}_{12}(\mu_3\text{-O})_{12}]$ core comprising a central $[\text{Mn}^{\text{IV}}_4\text{O}_4]^{8+}$ cubane held within a nonplanar ring of eight Mn^{III} ions by eight $\mu_3\text{-O}^{2-}$ ions. Peripheral ligation of complex **3** is proved by sixteen μ_2 -carboxylate groups and four H_2O ligands. The Mn-O bond distances make it clear that all of the atoms in the central cubane are Mn^{IV} ions, while the ring consists of eight Mn^{III} ions. These assignments supported by the marked Jahn-Teller elongation of the axial Mn-O bonds (2.093-2.260 Å), which are on average 0.255 Å longer than the

analogous equatorial Mn-O bonds (1.873-2.012 Å). Complex **3** has one H_2O ligand on each of four Mn^{III} ions; Mn(4), Mn(6), Mn(4A), and Mn(6A) which are bonded to two Mn^{IV} ions via two $\mu_3\text{-O}^{2-}$ ions.

(a)



(b)

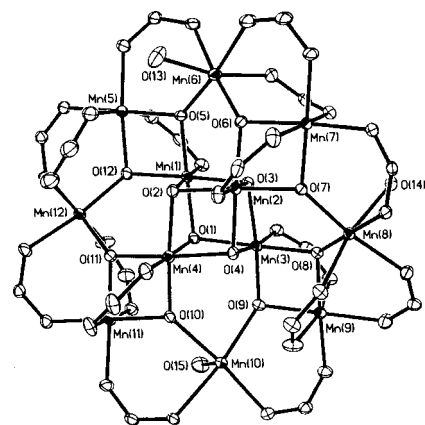


Figure 1. (a) Molecular structure of complex **3** and (b) molecular structure of the anion of complex **4**. The ClH_2C -groups of the acetate ligands, PPh_4 ion, the H_2O and CH_2Cl_2 solvate molecules are omitted for clarity.

An ORTEP plot of the anion of **4** is shown in Figure 1(b). The structure shows that the single added electron produces a valence trapped $\text{Mn}^{\text{II}}\text{Mn}^{\text{III}}_7\text{Mn}^{\text{IV}}_4$ anion rather than a $\text{Mn}^{\text{III}}_9\text{Mn}^{\text{IV}}_3$ ion. Compared to complex **2**,² complex **4** has one interesting feature. Unlike complex **2**, complex **4** has only three bound H_2O ligands, Mn(10) being five coordinate with one H_2O ligand. The other two H_2O ligands are bonded to Mn(6) and Mn(8), which is bonded to two Mn^{IV} ions via two $\mu_3\text{-O}^{2-}$ ions. For Mn(10) atom, the equatorial Mn-O bond lengths show a pronounced elongation (2.070-2.188 Å) relative

to the corresponding bond distances (1.860–1.989 Å) for the Mn^{III} ions. Clearly, the Mn(10) atom in complex **4** is a Mn^{II} ion, and it does not exhibit a Jahn-Teller distortion as seen for all the Mn^{III} ions in the complex **3**.

Variable-temperature dc magnetic susceptibility data were collected for polycrystalline samples of complexes **3** and **4** in an applied field of 1.0 kG, and in the temperature range 2.00–310.0 K, which were measured by a SQUID magnetometer (Quantum Design, MPMS-7).¹⁰ The samples were embedded in eicosane wax to prevent any torquing of the polycrystalline in the magnetic field. Pascal's constants¹¹ were used to estimate the diamagnetic corrections and to give the values of -1.06×10^{-3} and -1.21×10^{-3} emu/mol for complexes **3** and **4**, respectively. As can be seen in Figure 2, for complex **3** μ_{eff} per molecule slowly decreases from $12.96 \mu_{\text{B}}$ at 310.2 K to $12.20 \mu_{\text{B}}$ at 170.2 K, and then increases, reaching a maximum of $18.43 \mu_{\text{B}}$ at 14.0 K, finally decreases to $8.19 \mu_{\text{B}}$ at 2.00 K. The data for the one-electron reduced complex **4** show similar temperature dependence; μ_{eff} per molecule slowly decreases from $12.39 \mu_{\text{B}}$ at 310.8 K to $11.55 \mu_{\text{B}}$ at 170.0 K, and then increases, reaching a maximum of $20.32 \mu_{\text{B}}$ at 11.99 K, finally decreases to $7.56 \mu_{\text{B}}$ at 2.00 K. This behavior is similar to that observed for complex **1**; which has a μ_{eff} values of $12.17 \mu_{\text{B}}$ at 300.0 K, with decreasing temperature increases to a maximum of $20.79 \mu_{\text{B}}$ at 15.0 K, whereupon there is a decrease to $15.79 \mu_{\text{B}}$ at 5.00 K.²

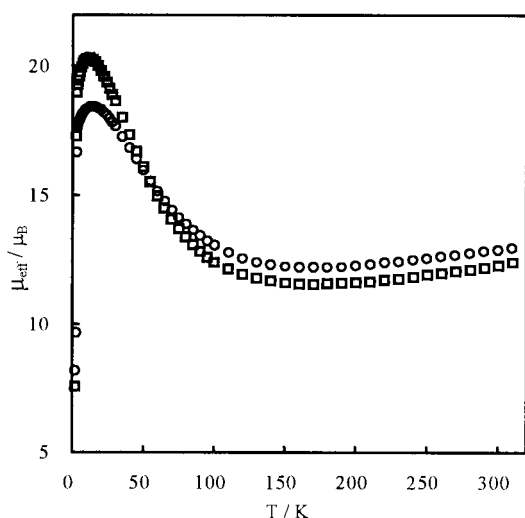


Figure 2. Plots of μ_{eff} versus temperature for polycrystalline samples of complex **3** (○) and complex **4** (□).

If there were no magnetic exchange interaction present in a Mn^{III}₈Mn^{IV}₄ and Mn^{II}Mn^{III}₇Mn^{IV}₄ complexes, then the spin-only effective magnetic moment with $g = 2.0$ should be $\mu_{\text{eff}} = 15.87 \mu_{\text{B}}$ and $\mu_{\text{eff}} = 16.22 \mu_{\text{B}}$ for complexes **3** and **4**, respectively. It is clear from the values of μ_{eff} per molecule for complexes **3** and **4** at 310.0 K that there are in both complexes appreciable exchange interactions present. The exchange interactions in the Mn^{II}Mn^{III}₇Mn^{IV}₄ complex **4** are greater than those in complex **3**, for the μ_{eff} per molecule for complex **4** at 310.0 K is much lower than its expected spin-only value compared to the Mn^{III}₈Mn^{IV}₄ complex **3**. The increase in μ_{eff} with decreasing temperature to a maximum at low temperatures is expected the fact that as the temperature is decreased only one high-spin

state is thermally populated. This Mn^{III}₈Mn^{IV}₄ complex **1** has been established to have an $S = 10$ ground state. Complexes **3** and **4** must have a ground state with a relatively large spin.

Reduced magnetizations and AC magnetic measurements are in progress to determine which total spin complexes **3** and **4** differ in their ground state. From primary results, they show frequency dependence in the out-of-phase AC magnetic susceptibilities and prove to be SMMs.¹² Furthermore, Mn₁₂ SMMs also exhibit steps on hysteresis loops, which are characteristic behaviors of magnetic quantum tunneling.^{1,13} The hysteresis loops measurements on complexes **3** and **4** will give insight into the mechanism of magnetization tunneling.

We thank the National Science Council of the Republic of China (NSC-89-2113-M-006-012) for support.

References and Notes

- R. Sessoli, D. Gatteschi, A. Caneschi, and M. A. Novak, *Nature*, **365**, 141 (1993); L. Thomas, F. Lioni, R. Ballou, D. Gatteschi, R. Sessoli, and B. Barbara, *Nature*, **383**, 145 (1996).
- R. Sessoli, H.-L. Tsai, A. R. Schake, S. Wang, J. B. Vincent, K. Folting, D. Gatteschi, G. Christou, and D. N. Hendrickson, *J. Am. Chem. Soc.*, **115**, 1804 (1993); A. R. Schake, H.-L. Tsai, R. J. Webb, K. Folting, G. Christou, and D. N. Hendrickson, *Inorg. Chem.*, **33**, 6020 (1994); H. J. Eppley, H.-L. Tsai, N. de Vries, K. Folting, G. Christou, and D. N. Hendrickson, *J. Am. Chem. Soc.*, **117**, 301 (1995).
- S. M. J. Aubin, N. R. Dilley, M. Wemple, M. B. Maple, G. Christou, and D. N. Hendrickson, *J. Am. Chem. Soc.*, **120**, 839 (1998).
- G. Aromi, S. M. J. Aubin, M. A. Bolcar, G. Christou, H. J. Eppley, K. Folting, D. N. Hendrickson, J. C. Huffman, R. C. Squire, H.-L. Tsai, S. Wang, and M. Wemple, *Polyhedron*, **17**, 3005 (1998).
- S. M. J. Aubin, Z. Sun, I. A. Guzei, A. L. Rheingold, G. Christou, and D. N. Hendrickson, *Chem. Commun.*, **1997**, 2339; D. Ruiz, Z. Sun, B. Albela, K. Folting, J. Ribas, G. Christou, and D. N. Hendrickson, *Angew. Chem., Int. Ed. Engl.*, **37**, 300 (1998); Z. Sun, D. Ruiz, E. Rumberger, C. D. Incarvito, K. Folting, A. L. Rheingold, G. Christou, and D. N. Hendrickson, *Inorg. Chem.*, **37**, 4758 (1998); Z. Sun, D. Ruiz, N. R. Dilley, M. Soler, J. Ribas, K. Folting, M. B. Maple, G. Christou, and D. N. Hendrickson, *Chem. Commun.*, **1999**, 1973.
- S. M. J. Aubin, S. Spagna, H. J. Eppley, R. E. Sager, G. Christou, and D. N. Hendrickson, *Chem. Commun.*, **1998**, 803; S. M. J. Aubin, Z. Sun, L. Pardi, J. Krzystek, K. Folting, L.-C. Brunel, A. L. Rheingold, G. Christou, and D. N. Hendrickson *Inorg. Chem.*, **38**, 5329 (1999).
- D. Gatteschi, A. Caneschi, L. Pardi, and R. Sessoli, *Science*, **265**, 1054 (1994); J. Villain, F. Hartman-Boutron, R. Sessoli, and A. Rettori, *Europhys. Lett.*, **27**, 159 (1994).
- Crystal data of complex **3**-3CH₂Cl₂·2H₂O: C₃₅H₅₀Cl₂₂Mn₁₂O₅₀, *FW* = 2709.93, monoclinic, space group *C2/c*, $a = 25.238(2)$, $b = 13.226(2)$, $c = 26.199(5)$ Å, $\beta = 94.761(13)^\circ$, $V = 8715(2)$ Å³, $Z = 4$, $D_{\text{cal}} = 2.065$ g/cm³, $R(R_w) = 0.0910(0.2776)$ (7645 unique reflections with $I > 2\sigma(I)$). Crystal data of complex **4**-2CH₂Cl₂·2H₂O: C₅₈H₆₆Cl₂₀Mn₁₂O₄₉P, *FW* = 2946.36, orthorhombic, space group *Fdd2*, $a = 51.3413(7)$, $b = 61.6796(7)$, $c = 12.8787(1)$ Å, $V = 40783.1(8)$ Å³, $Z = 16$, $D_{\text{cal}} = 1.919$ g/cm³, $R(R_w) = 0.0490(0.1204)$ (22937 unique reflections with $I > 2\sigma(I)$).
- T. Lis, *Acta Cryst.*, **B36**, 2042 (1980).
- Satisfactory elemental analysis data (C, H, Mn) were obtained. Anal. **3**·7H₂O; Found: C, 15.58; H, 2.08; Mn, 25.24%. Calcd. for C₃₂H₅₄Cl₁₆Mn₁₂O₅₅; C, 15.21; H, 2.14; Mn, 25.90%. Anal. **4**·3H₂O; Found: C, 24.11; H, 2.32; Mn, 23.10%. Calcd. for C₅₂H₆₄Cl₁₆Mn₁₂O₅₀P; C, 24.07; H, 2.31; Mn, 23.59%.
- "Theory and Application of Molecular Paramagnetism," ed. by E. A. Boudreaux, and L. N. Mulay, J. Wiley & Sons, New York (1976).
- H.-L. Tsai, T.-Y. Jwo, C.-S. Wur, G.-H. Lee, and Y. Wang, unpublished results.
- J. R. Friedman, M. P. Sarachik, J. Tejada, J. Maciejewski, and R. Ziolo, *J. Appl. Phys.*, **79**, 6031 (1996); J. R. Friedman, M. P. Sarachik, J. Tejada, and R. Ziolo, *Phys. Rev. Lett.*, **76**, 3830 (1996).